SCHLIEREN PHOTOGRAPHY OF THERMAL PULSES IN LIQUID He^4

A. I. GULYAEV

Institute for Physics Problems, USSR Academy of Sciences

Submitted January 30, 1969

Zh. Eksp. Teor. Fiz. 57, 59–73 (July, 1969)

Optical inhomogeneities (instantaneous fields of the density gradient) excited in liquid helium (at T = 1.3–2.3°K and saturated vapor pressure) as a result of a single pulse of Joule heat in a thin heater have been photographed by means of a Toepler apparatus. The changes in the structure of the sound wave packets as a function of the temperature and heat flux density are illustrated, and pictures showing mutual transformation of cylindrical waves of first and second sound at the vapor-liquid boundary in He II are obtained.

AMONG the various methods of study of the properties of liquid helium, the optical methods have been very little used. The basic experimental evidence on the mechanism of heat propagation in HeII in the experiments of Kapitza[1] with steady heat flow, and also in subsequent papers[2-4] with temperature waves were obtained by means of resistance thermometers. The use of such thermometers in the study of heat pulses in liquid helium[3,4] does not furnish a complete picture of the perturbations, inasmuch as the thermometers do not react on the sound oscillations of the liquid and observation of temperature waves ("second sound") is complicated by the local position of the thermometer, by the averaging of the temperature over its surface, and by distortions of the pulse shape. The piezoelectric crystals used for measurement of sound oscillations in helium are not sensitive to second sound. The investigation of the fields of the index of refraction of liquid helium by optical methods (with short light flashes) allows us to obtain information (practically instantaneously and without effect on these fields) on the spatial structure of all the interactions associated with change in the helium density.

The existence of density changes in a packet of second sound was shown in the work of the author[5] by means of the Schlieren method (Toepler method). This also made it possible to see the temperature waves in HeII by this method. In the work mentioned, experiments were described with this same method used in an improved cryostat prepared for the study of two problems: 1) to make clear the structure of the perturbations which arise in liquid helium as the result of a pulse of Joule heat in a thin plane heater (without backing) which made contact only with the liquid and which was located far from the walls parallel to it, in order to avoid interference with excitations reflected from it, and 2) to obtain a picture of the transformation of waves of first and second sound at the vapor-liquid boundary.

1. SENSITIVITY OF THE METHOD

It is useful to estimate the limiting sensitivity of the Schlieren method in the apparatus used, inasmuch as it is difficult to obtain quantitative characteristics of the perturbations by this method. In the Toepler apparatus IAB-451 with a mirror-meniscus optical system,[6] the relative change in the illumination along the image of the optical inhomogeneity (Schlieren) is equal to $A \sim \beta f/a$. where β is the angular declination of the ray passing through the screen, f = 1917 mm the focal length of the optical system, and a the distance between the edge of the Foucault knife edge and the edge of the image of the illuminated slit. If we assume that, as a result of the brightness of the light flash (~ 1 μsec) one can obtain a Schlieren image on a photo film for a = 0.025 mm, and that for reliable observation it is necessary that $A_0 \approx 0.15$, then the smallest recordable declination of the rays will be $\beta_0 = A_0 a/f \approx 2 \times 10^{-6}$ rad. (In the best apparatus, one achieves $\beta_0 = 0.5 \times 10^{-6}$ cm, see[6], p. 28.)

The light rays passing perpendicular to the plane layer of material under study (h is the thickness of the layer, n the index of refraction, and the x axis is in the plane of the layer) undergo an angular deflection $\beta \approx h(dn/dx) = h(dn/d\rho)d\rho/dx)$. The specific refraction of the liquid helium in the temperature range 1.5–4.2°K does not depend on temperature ([7], p. 39) and from the Lorenz-Lorentz formula one can obtain $dn/d\rho = (n^2 + 2)(n^2 - 1)/6n\rho \approx (n - 1)/\rho \approx 0.20$ cm^2/g for the entire temperature range. Consequently, in the entire interval, the apparatus preserves a constant sensitivity to changes in the density gradient. For a layer thickness h ≈ 60 mm (n = 1.029, $\rho \approx 0.145$ g/cm^3) the smallest distinguishable density gradient of helium will be $(d\rho/dx)_0 = \beta_0\rho/(n - 1)h \approx 1.5 \times 10^{-6}$ g/cm^4, and for the relative density $(d\rho/\rho\, dx)_0 \approx 10^{-5}$ cm^{-1}. In a sound wave, such a change in density corresponds to a pressure gradient $(dP/dx)_0 = u_1^2(d\rho/dx)_0 \approx 800$ dynes/cm^3, while this limiting value also depends weakly on the temperature. Finally, the smallest distinguishable temperature gradient $(dT/dx)_0 = d\rho/dx)_0/\rho\alpha$ increases with decrease in the temperature as a consequence of the decrease in the coefficient of thermal expansion $\alpha = -(\partial\rho/\partial T)_P/\rho$; near T_λ in He II we have $(dT/dx) \approx 3 \times 10^{-4}$ deg/cm, and for T = 1.50°K we get $(dT/dx)_0 = 5 \times 10^{-3}$ deg/cm.

In operation with liquid helium, there is a unique possibility of testing the sensitivity of the apparatus in practice. Convective streams of heated liquid, directed downward in the gravitational field ($\alpha > 0$), can exist in helium only inside an interval of 0.006°[8,9] between the temperature T_ρ = 2.178°K, where the density of the

liquid (under pressure of saturated vapor) reaches a maximum and $\alpha = 0$, and the temperature of the λ transition $T_\lambda = 2.172°K$, when convection in the liquid is completely absent. The greatest change in the density between the extreme points of this interval does not exceed $d\rho \approx 5.9 \times 10^{-6}$ g/cm^3. Since $0 < |\alpha| < 2 \times 10^{-2}$ inside this interval, and convective streams do not develop simultaneously over the entire thickness of the liquid layer, observation of such streams is evidently possible if $(dT/dx)_0 < 10^{-3}$ deg. The check described in Sec. 3 revealed the sensitivity to be close to what was expected.

2. EXPERIMENTAL TECHNIQUES AND APPARATUS

The scheme of the apparatus is pictured in Fig. 1. A cryostat with plane-parallel glass windows of diameter 230 mm was placed between the collimator 1 and the sighting tube 10 of an IAB-451 telescope[6]. The input slit 2 of the apparatus, of width $b \approx 50$ μ and length 4 mm was illuminated by a xenon strobe lamp 3 (the lamp ISSh-100-3, operating potential 6 kV, discharge energy 10 J, brightness amplitude $\sim 10^6$ cand/cm^2, duration of intense light of the discharge ~ 1 μ sec). The beam of parallel rays passing through the window of the cryostat and the liquid helium is collected at the focus of the sighting tube, where the image of the slit is partially overlapped by the opaque knife-edge 11, the edge of which is set parallel to the edge of the image; the open part of the image of the slit a changes from 30 to 2 μ. The image of the studied layer of liquid is projected on a 36 mm film with the help of an auxiliary objective. The angular declination β of the light ray on the Schlieren leads to a displacement of it at the focus relative to the knife edge and consequently the degree of coverage of this ray by the knife edge is changed and hence the illumination of the image of the layer (which corresponds to the location of the Schlieren) is changed. A narrow slit source of light allows the recording of very small declinations of the rays for sufficient illumination ($\sim 10^{-6}$ rad), but only in the direction perpendicular to the slit. Decrease of the value of a increases the sensitivity of the apparatus, but with decrease in the ratio a/b, all the more essential parts of the diffraction picture of the image of the slip are covered; therefore distortions increase in the investigated pictures: the dimensions of the Schlieren image are partially changed, the bright radiation of the opaque knife edge parallel to the slit, develops. In view of this, the width of the gap becomes as small as possible, and the characteristic Schlieren pictures are reproduced several times and photographed for different values of a. Glass disks for the windows of the cryostat were prepared from Kron-8 optical glass with plane-parallel surfaces (deviations from planarity when unloaded was not more than 0.3 μ); the thickness of the loaded disks was chosen to be 25 mm for reasons of rigidity.

The cryostat consisted of an exterior jacket 4 with windows 5, inside which were suspended on stainless steel pipes, in the common vacuum space, a bath with liquid nitrogen 19, a bath with liquid helium 20, and the working chamber 9. Glass disks 8 were attached to the framework of the chamber, which was made of stainless steel, on circular copper washers of rhombic

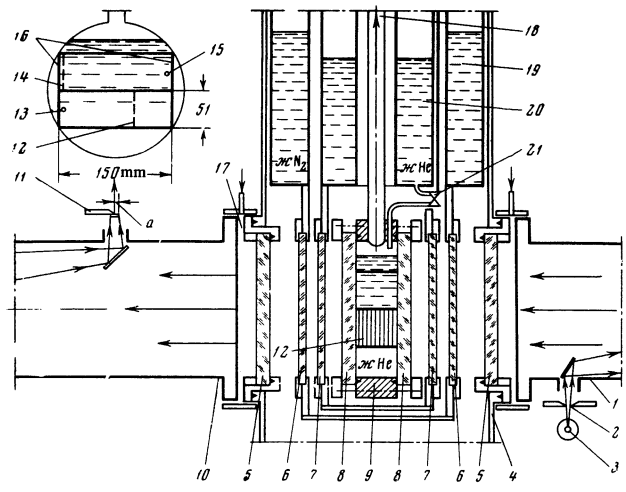

FIG. 1. Schematic drawing of apparatus (explanation in text).

cross section. A layer of liquid helium is poured between these disks. The liquid is introduced into the chamber from the helium bath through the valve 21; the gaseous helium is cooled along the tube 18, which is also used to bring the electrical leads into the chamber. The surface of the disks 8 is shielded from thermal radiation by the glass disks 7, which make contact with the helium bath. The chamber and the helium bath are surrounded by a nitrogen bath with a copper screen, the windows in which are covered by glass disks 6.

The external window disks 5 are sealed with circular washers of indium. Under operating conditions, the temperature of the external surface of the disks 5 often falls below the dew point of the surrounding air. In order to prevent condensation of moisture on the surface of the disks, the space 17 between the cryostat and the Toepler apparatus is fed a small amount of condensing nitrogen, which is brought in from the nitrogen bath. In spite of preliminary warming of the nitrogen and the mixing of it, which takes place in the space, considerable success was sometimes achieved. To avoid condensation of "dirt" on the cold optical surfaces inside the cryostat, the evacuated volumes were shielded by traps, and the filling of the working chamber after its pumping out in the heated state was only by the evaporated liquid. Preliminary cooling of the cryostat takes place at a rate not greater than 15°/hour, first by liquid nitrogen, then by gaseous and liquid helium. In the steady operating state, the total flow of heat into the helium chamber was equal to ~50 mW.

Inside chamber 9, two working volumes, in the form of parallelepipeds with dimensions (in the cold state) $56.6 \times 60 \times 150$ mm (upper) and $5.2 \times 60 \times 150$ mm (lower) were separated by means of three horizontal and two vertical plane walls 16, made of plastic; the spaces between the edges of the walls and the glass disks were increased in cooling to 0.3 mm. Flat heaters 12 and 14 and cylindrical heaters 13 and 15 were attached to the walls. All the heaters were made of annealed constantan ribbon of thickness 0.02 and width 0.47 mm, located along the surface of the heater with a spacing of 1 mm. The ribbon took up 50% of the nominal surface of the heater, and the area of the metal

surface washed by the liquid (from the two sides of the ribbon) is approximately equal to the area of the nominal surface of the heater, to which will be related the characteristic dimensions. The mass of the constantan in the heaters amounted to $g = 9$ mg/cm^2. The cylindrical heaters 13 and 15 were coiled from the ribbon in the shape of a helix of diameter 2.6 mm and length 58 mm, suspended in a horizontal position on glass rods near the vertical walls; the projection of these cylinders on the photographs have the form of circles with a line thickness ~0.3 mm.

The heater 14 consists of horizontal pieces of ribbon, stretched along the surface of the left vertical wall and hung by "pins" on the edge of the external side of the wall. The surface of the heater 12 was 50 mm from the right wall and was formed of vertical strips of ribbon, going out from the working volume across a space of width ~0.1 mm to the inside the hollow formed by the horizontal walls, where the strip hangs from the pins. Inside these hollows is 13% of the total length of ribbon. In the pictures, the plane of the heater 12 is seen as straight lines of thickness ~0.15 mm.

The projections of (well-prepared) heating surfaces in the form of thin lines are obtained as the result of the orientation of the chamber relative to the optical axis of the apparatus. To test the orientation, light rays were employed that were visible for the correct setting of the chamber across the mutually perpendicular gaps of width 0.2 mm and length 60 mm (the gaps were formed at the joints of the opaque walls inside the chamber). The optical axis of the apparatus is horizontal, i.e., parallel to the free surface of the liquid.

Heat is released in the heater in the passage through it of a single "rectangular" pulse of electric current. After a time interval t_+ following the beginning of the pulse, a light flash is ignited in the Toepler apparatus, which also records the picture of the perturbation produced by the heat pulse. For synchronization of the pulse and the light flash, a generator of shifted rectangular pulses with smooth regulation of amplitude, pulse length $t = 0.5$–2000 μ sec) and delay (0–2000 μ sec) is used. The heater (anode load of lamp) is fed by an amplified support pulse, the amplitude and shape of which are controlled at the screen of the electron oscillograph (current amplitude to 1.6 A, rise time of fronts ≤ 0.3 μsec, slope of "horizontal" part $\leq 5\%$).

The shifted pulse of the generator enters into the assembly with stepwise regulation of the delay (up to 0.2 sec in steps of 2 msec) and then, after amplification, is fed to the firing electrode of the ISSh-100-3 tube and initiates the discharge.

The time interval between the beginning of the

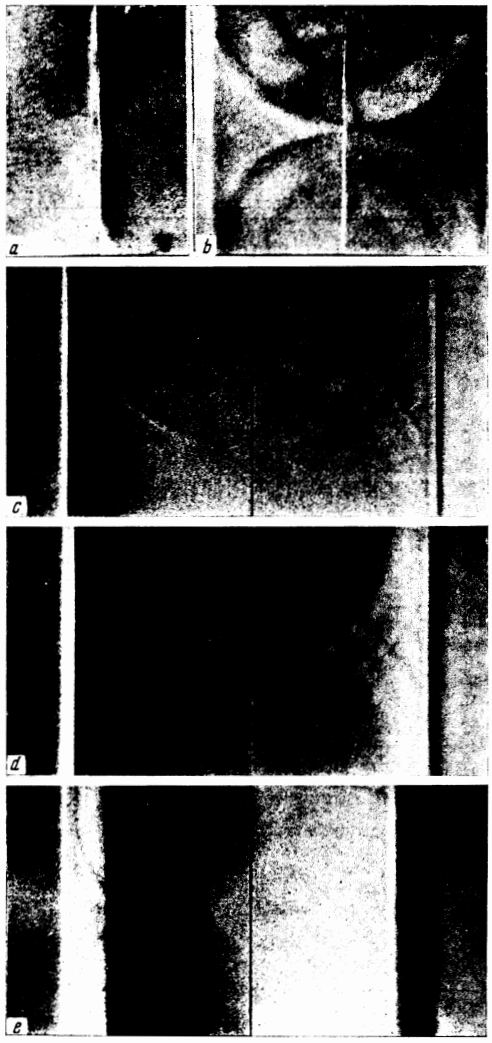

FIG. 2. Convective streaming of liquid for $T_\lambda < T < T_\rho$ (a) and packets of sound wave (b–e) in He I (see text and Table).

Figure	T, °K	N, W/cm^2	t_*, μsec	t_+, μsec
	Fig. 2			
a	2.174	10^{-4}	—	—
b	2.22	2.5	8	130
c	2.20	3.2	8	182
d	2.18	3.2	20	183
e	2.171	3.2	50	182
	Fig. 3			
a	2.167	3.2	50	213
b	2.164	3.2	50	224
c	2.161	3.2	50	209
d	2.158	3.2	50	209
	Fig. 4			
a	2.161	3.2	50	176
b	2.152	3.2	50	176
c	2.125	3.2	50	212
d	2.026	3.2	1500	2017

Figure	T, °K	N, W/cm^2	t_*, μsec	t_+, μsec
	Fig. 5			
a	2.100	3.2	1500	2508
b	2.22	3.2	20	345
c	2.067	18	50	178
d	1.866	18	50	597
e	1.880	18	50	1352
f — *i*	1.68	18	50	685—832
j	1.885	18	100	960
k	1.736	18	20	112
l	1.747	18	20	299
m	1.755	18	20	617

pulse in the heater and the moment of the light flash is measured by electronic counting apparatus with time markers of 0.1 μsec (a temperature-stabilized quartz with a resonant frequency of 10 MHz). The leading edge of the pulse in the heater triggers the light of the markers, which is established by luminous discharge between the principal electrodes of the ISSh tube (the light is not established by the igniting pulse). The error in the measurement of the interval t_+, due principally to the curvature of the fronts and some indeterminacy of the time of lighting of the discharge did not exceed 1 μsec. The smallest interval in the applied system of synchronization is equal to ~3 μsec. The triggering of the entire system takes place at the instant of opening of the shutter of the photo-apparatus.

The resolving capability of the photographs, reduced to natural dimensions, amounts to 0.1 mm; the shift of the perturbations which have the velocity of sound, within the time of illumination of the discharge, is equal to 0.2—0.3 mm; finally, an error up to 0.5 mm can arise in the determination of the boundary of the perturbation. Therefore even in enlarged drawings, the measurements of distances traveled by the sound perturbations in the interval t_+ can reach 0.6 mm and in the case of fronts of second sound, do not exceed 0.2 mm.

The temperature of liquid helium in the chamber was determined from the vapor pressure (1958 scale) with an error not greater than 0.001 deg. The helium pressure in the chamber was measured by a calibrated double gauge membrane manometer reading 0.02—0.05 mm Hg per division. To maintain the temperature at 1.25—1.30°K, the helium was pumped from the chamber by a continuous mechanical vacuum pump; sometimes it was more convenient to make the observations at higher temperatures while slowly increasing the pressure in the closed chamber (quieter state of the vapor above the liquid and absence of vibration from the pump).

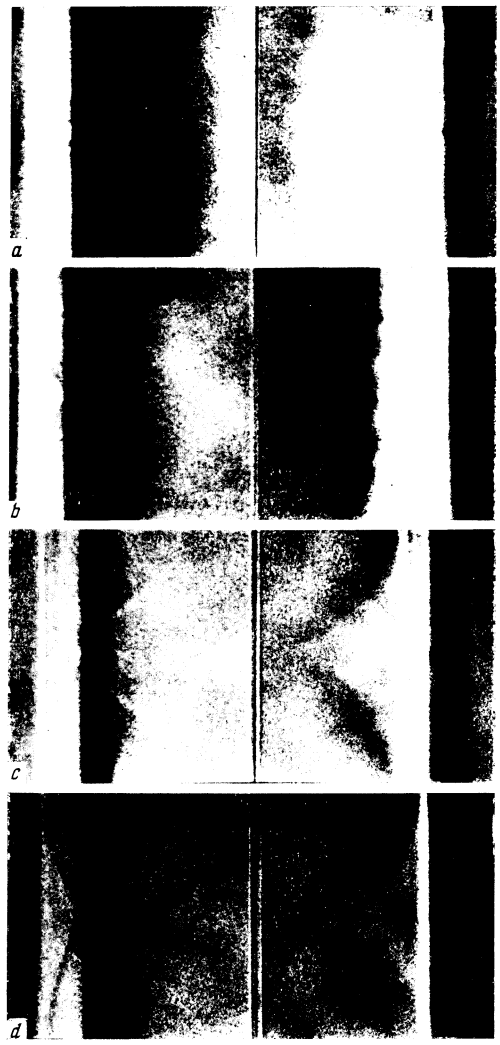

FIG. 3. Waves packets of first and second sounds in He II near T_λ. The vertical line in the middle of the photographs is the projection of the heater 12 of height 51 mm.

3. RESULTS OF OBSERVATIONS

In Figs. 2—5 we show Schlieren photographs of perturbations formed in liquid helium (at saturated vapor pressure). Figures 2—4 were obtained upon the release of Joule heat in the flat heater 12, the projection of which is seen as a thin vertical line in the middle of the photographs. The length of this line, i.e., the thickness of the layer of liquid between the horizontal walls, is equal tp 51.2 mm. The slitted light source in the Toepler apparatus was also located vertically (the horizontal projections of the density gradient are therefore recorded); the light discharge lasted ~1 μsec. The location of the edge of the Foucault knife edge was so chosen that the amplification of the illumination of the part of the drawing in comparison with the "zero" gray tone corresponded to the positive direction (left to right) of the density gradient of the liquid on this part. The connection between the direction of the gradient and the change in the illumination can be established by the convective motion of the heated liquid in the field of gravity, shown in Fig. 2a. the observation of convection inside the interval of temperatures between the maximum density (T_ρ = 2.178°K) and the λ point (T_λ = 2.172°K) can also serve as a test of the sensitivity of the apparatus (see Sec. 1).

Figure 2a shows the photograph of convective streaming directed downward along the heating and flowing along the lower horizontal wall (an increase in the liquid density close to the heater). The streams appear as the result of a stationary emission of heat in the heater with current density $W \leq 0.12$ mW/cm². Increase in W at the same temperature of the liquid far from the heater (T = 2.174°K) disrupts the stable flow and for W = 0.8—1.0 mW/cm² an intense turbulent convection is observed with streams directed principally upward because of the local heating of the liquid above T_ρ. In the case of small fluxes (~0.05 mW/cm²) the helium temperature at which the direction of convection changes is equal to 2.177°K. The determination of the temperature of the λ transition from the instants of the phenomenon and the disappearance of convection gives T_λ = 2.172 ± 0.0007°K.

In the experiments described below, the heat in the

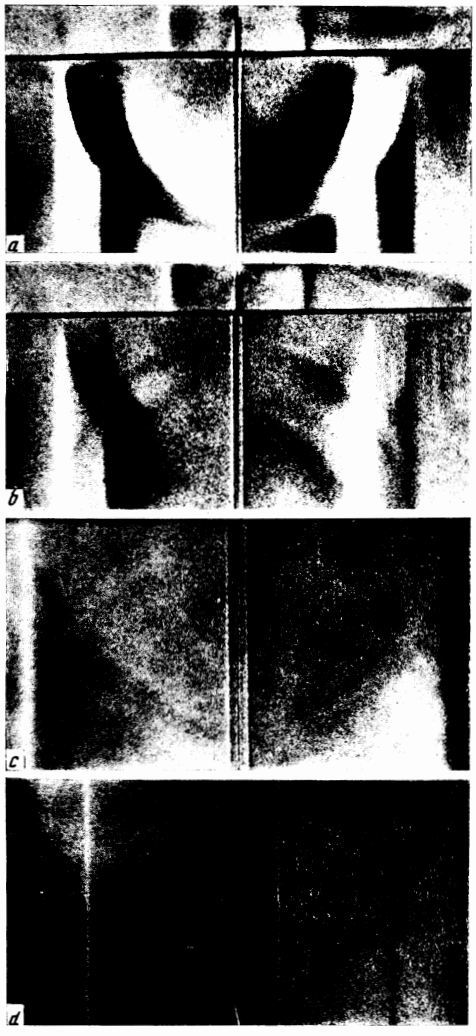

FIG. 4. Packets of first and second sounds in He II. In photographs a and b, the heater 12 intersects the vapor-liquid boundary.

heater is emitted as the result of the passage of a single rectangular current pulse with length t_*, rise time $\leq 0.3\ \mu$ sec, and electric power (in the pulse) N, computed per unit area of the normal surface of the heater (for the flat heater 12, this is the area occupied by the cross section of the liquid column). The light flash is fired after a time t_+ reckoned from the leading edge of the pulse. The values of N, t_*, t_+ and T which characterize the photographed processes, are shown in the table.

In the range $T \gtrsim T_\lambda$, the current pulse in the heater (constant ribbon of thickness 0.02 mm and mass $g \approx 9$ mg/cm^2) produced appreciable perturbations in the liquid in those cases in which the power was $N \geq 2.5$ W/cm^2 and the energy released amounted to $Nt_* \geq 15\ \mu$J/cm^2 (see Fig. 2b). At smaller values of N and Nt_* we succeeded in noting only a weak convective stream of liquid, which developed several seconds after the pulse. When $N \geq 3$ W/cm^2, the excitations acquired sharp boundaries and are reproduced exactly. Figures 2c–2e illustrate the change in the perturbation picture with increase in the pulse length (8.20 and 50 μsec). Lowering of the temperature of the liquid in these photographs from 2.27 to 2.172°K and the ensuing change of the sign of the coefficient of thermal expansion α do not show any appreciable effect on these processes. A reverse change in the illumination on the images of the perturbations along the different sides of the heater showed that these density gradients have the opposite directions, i.e., that the process is completely symmetric relative to the plane of the heater.

On the pictures of the process obtained for any one value of a (see Sec. 2), the parts with increased illumination contain greater detail than the darker parts, but for other positions of the Foucault knife edge details are also revealed in the dark portions. The heater, made of metallic ribbon, excites a number of cylindrical streaks (Schlieren) on the edges of the ribbons, which then combine into a "quasiplane" perturbation and the traces of which are easily visible

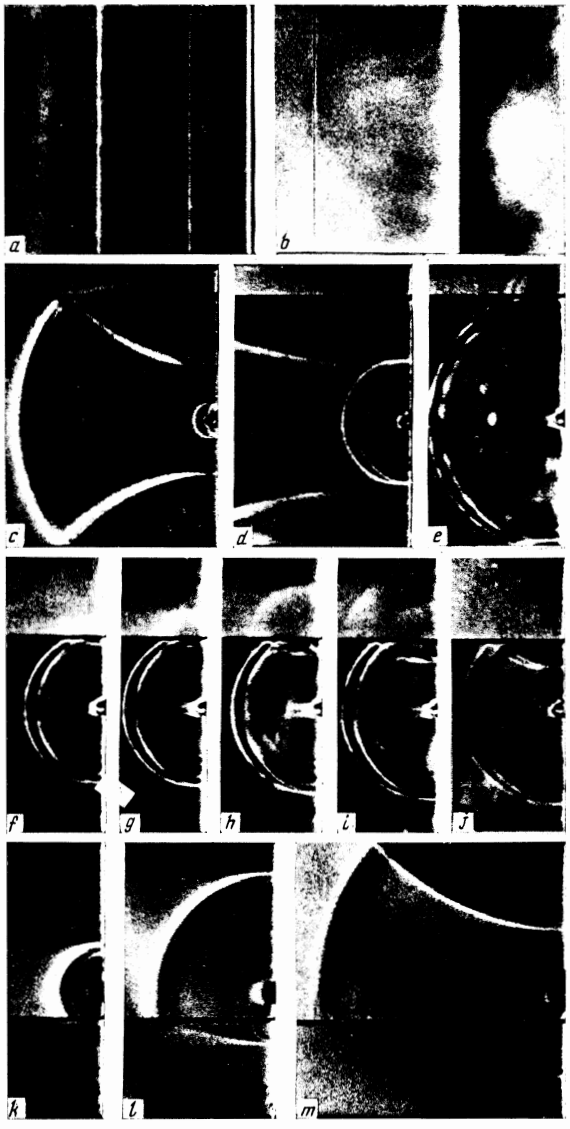

FIG. 5. Transformation of cylindrical waves of first and second sounds at the vapor-liquid boundary in He II (c-m). The curves at the right side of the photographs are the projection of the heater 15.

when the ribbons are located perpendicular to the plane of the image (heater 14, see the photograph in[5]). If the ribbons are stretched parallel to the plane of the image, as is done for the heater 12, then no multiple streaks are seen, but a comparison of the pictures obtained following simultaneous application of identical pulses in heaters 12 and 14 shows that the "plane" excitations in this case have very much the same structure. The subsequent description applies only to such features of plane perturbations which do not depend on the direction of the ribbons in the heaters.

In order to determine the rate of propagation of the perturbations and the moment of their formation, the distances l from the heater to the characteristic limits of visible Schleiren streaks were measured on the enlarged pictures, obtained for the same temperature and different values of t_+. These are plotted in the form of points in coordinate system t_+ and l. Points corresponding to the initial boundaries of the Schlieren are located along straight lines whose slope gives the rate of propagation, while the intercept of the lines with the t_+ axis gives the time of formation of the boundary.

All the excitations in Figs. 2c-2e leave the heater with the velocity of sound in the liquid (219, 217 and 216 m/sec), and their visible leading edges appear 3–4 μsec after the beginning of the electrical pulse. From the moment of formation near the heater, each sound perturbation propagated in the liquid without appreciable change in its structure. During the time t_* of the current flow along the heater in the liquid, the plane region of the perturbation, whose visible leading edge begins with an increase in density independent of the sign of α, grows. The illumination of the image of this region indicates an increase in its density, and after the conclusion of the electrical pulse the sign of the density gradient changes in reverse fashion. Following the leading edge inside this region, two bands appear with opposite signs of the gradient, indicating the presence of oscillations with wavelength 0.8–1.6 mm. At constant power N and $t_* > 5$ sec, the structure of the "sound packet" formed in the time t_* is reproduced independently of the value of t_*. After the flow ceases, a region of gradual decrease in the density appears, the extent of which depends strongly on t_* and amounts to 50 mm for $t_* = 50$ μsec (Fig. 2e).

The approximate density distributions of the liquid are shown in Fig. 6 (in arbitrary units relative to the equilibrium value of ρ) in perturbations that are propagated a distance l to the right from heater 12 in the time $t_+ = 200$ μsec. It must be noted that these distributions are sketched (with account of the condition of mass conservation) only on the basis of the field of the density gradient existing in the photographs, the quantitative data on which have only an approximate character.

The photographs in Fig. 3 illustrate the changes in the gradient fields with decrease in temperature below T_λ for constant N = 3.2 W/cm^2 and $t_* = 50$ μsec. The first (and unexpected) sign of the changing state of the liquid is the appearance at the end of the sound perturbation of a new front of width 1–2 mm, on which the density gradient again changes sign (the "secondary" compression front). In Fig. 3a, this front is at a distance of 8–10 mm from the heater and is bent to the left. With decrease in temperature (by 0.003°, Fig. 3b, c, d) the secondary front becomes more distinct; it appears close to the sound packet and initially amplifies the oscillations at the back of the packet (Fig. 3c), and at T = 2.158°K (Fig. 3d) it becomes superimposed on the sound packet, weakening its trailing edge. In the density distributions of Fig. 6, the place of the sign change in the gradient, corresponding to the secondary front, is indicated by the vertical arrows. From the moment of appearance, this front moves together with the sound packet, but inasmuch as its position relative to the packet depends strongly on the temperature, the scatter of the measured values of its velocity about the sound velocity reaches 20%. If we take the velocity of this front to be equal to the sound velocity u_1, then the time necessary for the appearance of the secondary front will be $t_0 = l_0/u_1$, where l_0 is the distance from the beginning of the sound packet to the secondary front, measured on the photographs (see also Fig. 6).

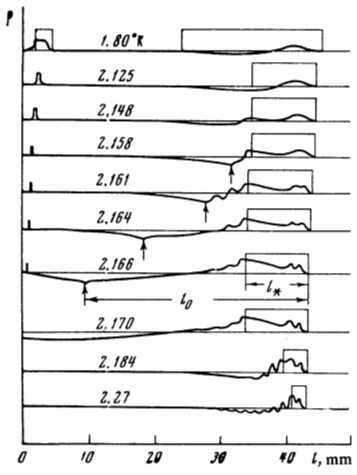

FIG. 6. Typical distribution of liquid density (in arbitrary units relative to the equilibrium value of ρ) at a distance l from heater 12 200 μsec after the beginning of the pulse.

Values of the interval t_0 are represented by the points in Fig. 7 as a function of the temperature of the liquid, for $t_* = 50$ μsec; the dashed curves in this drawing show the most probable values of the interval t_0 for $t_* = 30$ μsec (curve b), and 20 μsec (c). The secondary front inside the sound packet, i.e., for $t_0 < t_*$, is not seen, but when the temperature of the

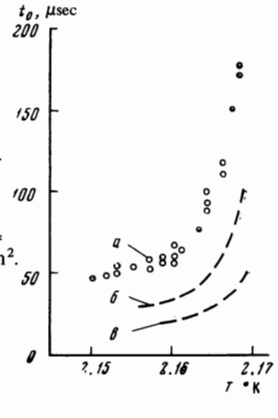

FIG. 7. Time interval t_0 from the beginning of the pulse to the moment of formation of the "secondary" front (see Fig. 3 and Fig. 6): a – t_* = 50 μsec, b – t_* = 30 μsec, c – t_* = 20 μsec; N = 3.2 W/cm^2.

liquid falls to this level, the clear fronts of the packet disappear, as is shown in Fig. 6, and at $T < 2.140°K$ ($N = 3.2$ W/cm^2) the sound perturbation represents an increase in the density with subsequent smooth decrease (see Fig. 4c), and the extent of this perturbation no longer depends on the pulse length if $t_* > 20$ sec. Further decrease in the temperature to 1.30°K at N = const does not change the structure of the sound wave, but it does increase to 10–12 μsec the delay between the initial electrical pulse and the moment of appearance of the visible boundary of the perturbation; the minimum energy that must be released in the heater to excite a visible sound wave also increases to $Nt_* = 30$ μJ/cm^2. In the case of no change in the curvature of the fronts of the electric pulse (0.3 μsec) and $N = 3.2$ W/cm^2, the acoustic frequencies excited by the heater in the liquid and reaching ~200 kHz near T_λ decrease to ~10 kHz with decrease in temperature.

Upon formation of the secondary front (Fig. 3), the perturbations in the liquid behind this front appear to be weak; a small growth in the density is noted in the direction of the heater, around which the boundaries appear of still another plane packet, which include the liquid of higher density and which leaves the heater with the velocity of second sound. It has not been possible to determine the delay of the instants of appearance of the leading and trailing edges of this packet relative to those of the electrical pulse. The boundaries of the packet of second sound are marked by distinct bands of width from 0.3 to 1.5 mm, on which the density gradient differs from zero; the width of the bands decreases with increase in temperature and increase in N. Inside the packet, even for pulse duration $t_* = 1500$ μsec (Fig. 4d) no change in density is noticeable. Measurements on the photographs, obtained for small values of $a = 2–5$ μ (Fig. 5a), show that the leading band is 1.5–2 times wider than the trailing one and the change of density in the packet of second sound has the form shown as an example in Fig. 6 at $T = 1.80°K$. A sharper change of density on the trailing edge, relative to the leading edge, also appears in the process of formation of the packet. In Fig. 5a, where the right boundary is formed by the heater 12, in addition to the distinct fronts of the packet of second sound, which has only just been separated from the heater and is moving to the left, a spreading band of sound perturbation is also visible, already twice reflected from the walls and again traveling in the same direction.

In addition to the plane packets, weak cylindrical sound waves are noted in Figs. 2c–2e and Fig. 3. These, as it was discovered, are excited on the lines of intersection of the plane of the heater 12 with the horizontal walls at the moment of breakaway of the departing plane fronts. The initial change of density in the cylindrical waves has the same sign as at the beginning of the excited plane fronts, and then the cylindrical band of opposite sign follows. The appearance of these waves is not connected in time with the action of the electrical pulse; they are excited even after cooling of the heater if distinct fronts are still separating from its plane. It is interesting to note that the motion of the packets of second sound from the plane of the heater is accompanied by the excitation of (weak) cylindrical waves of second sound on this same line.

A curious phenomenon is observed when the plane of the heater intersects the vapor-liquid boundary. On the line of intersection of these planes at $T < 2.15°K$ a weak cylindrical wave (Fig. 4b) is also created under similar conditions, but the change in density in it has the opposite sign in comparison with the departing plane front. If $T \geq 2.16°K$ and the sound packet is intense (around T_λ and higher) the cylindrical wave excited on this line is seen to be commensurate in intensity with the plane packet, which strongly changes the observed picture (Fig. 4a). A sharp decrease in the intensity of the cylindrical wave is steadily observed upon decrease in the temperature from $T = 2.16°K$ by not more than 0.01° (see photographs a and b in Fig. 4). In Fig. 5b, the right-hand boundary of the photograph is the image of the wall from which the plane sound packet is reflected (and moves to the left); it is seen that in the reflection of the packet from the walls the cylindrical waves are not excited at the edges of the angles.

Part of the heater 12 which emerges through the free surface of the liquid into the vapor (Fig. 4 a and b) excites compressional sound waves in the vapor phase during heating. In their structure, these recall the sound waves in the liquid at $T < 2.14°K$, for example, in Fig. 4c (the trailing edge of the perturbation is either very weak or completely absent). The sound velocity in the vapor increases significantly even at a distance of several centimeters from the surface of the liquid.

Measurement of the distances l traversed by the excitations in time t_+ permits us to determine the velocities of propagation of first and second sound in the liquid and of sound in the vapor. The error of measurement of l did not exceed 0.6 mm while the motion of the perturbations could be traced up to $l \leq 1000$ mm in the case of multiple reflections. The error of measurement of the interval t_+ was no greater than 1 μsec even for $t_+ = 10^5$ μsec. Therefore, the basic errors in the measurements were due to the dependence of the velocities on the temperature and to nonlinear effects. The values obtained for the sound velocity in the liquid agree with the data of Atkins and Chase;[10] the velocity of second sound, with corrections for the large amplitude, differs little from its value in the work of Peshkov,[11] reduced to $T_\lambda = 2.172°K$. It is convenient to list here only certain values of the sound velocity in the vapor, measured as the wave packet moves along the free surface of the liquid: 71.75 ± 0.05 m/sec for $T = 1.33°K$, 80.30 m/sec for $T = 1.882°K$ and 83.80 m/sec for 2.10°K.

For observation of wave transformations on the vapor-liquid boundary, cylindrical waves that were more intense than the plane waves and had a variable angle of incidence were excited. The surface of the cylindrical heater 15 almost touched the vertical wall and the right side of the excited wave, reflected from the wall and undergoing scattering at the surface of the heater, propagates behind the left side of the wave. Behind the leading compressional edge in such a wave, there is a region of diminishing density; the trailing edge does not appear in cylindrical waves. In Fig. 5c,

the acoustic front of the compression, together with the reflected wave, travel to the left from the heater to a distance of 39.5 mm, and part of it is reflected below from the horizontal wall in the form of compressional waves, and from the vapor-liquid boundary in the form of rarefaction waves. In the vapor above the surface of the liquid, a compressional wave is clearly evident, formed as the result of the refraction of the wave in the liquid, although the transformation coefficient in this case is very small, in agreement with the calculations of Chernikova.[12]

Upon reflection of the cylindrical wave from the lower wall, a refracted wave is formed in the (plastic) material of the wall; this wave which moves along the wall with a velocity greater than u_1 and which emerges again in the liquid, exciting a lateral wave. In Fig. 5c, part of the lateral wave is seen as a bright band, tangent to the reflected wave and traveling to the left at the acute angle φ to the horizontal wall. Measurement of the angle φ gives the possibility of determining the sound velocity u by such a method in nontransparent materials submerged in liquid helium, inasmuch as $u = u_1/\sin\varphi$. For $T = 2.0^\circ K$, the sound velocity in the plastic, computed by such a method, amounts to 1150 m/sec, and in organic glass it amounts to 710 m/sec.

An interesting phenomenon is observed in Fig. 5c. The incidence of the compressional wave from the liquid on the vapor-liquid boundary is accompanied, in addition to reflection and refraction, by an excitation (at the moment of incidence) of "secondary" cylindrical rarefaction waves on the line of intersection of the boundary with the vertical wall. The secondary wave in the liquid, having the form of an arc of a circle and being tangent to the wave reflected from the boundary at the wall, is easily seen in Fig. 5c. The secondary wave in the vapor is tangent to the refracted wave, but is scarcely visible in the photographs. It is useful to observe that in the reflection of the wave in the liquid from the corner formed by the walls (for example, from the right vertex corner in Fig. 5c, when the level of the liquid is higher than the wall), the secondary cylindrical wave is not excited. If there is a gap in the corner between the solid walls (width 0.2 mm and depth 1.5 mm; on the right lower corner in Fig. 5c), then a similar picture is observed but here several secondary waves are formed.

The cylindrical wave of second sound is reflected from the walls (see Fig. 5c, 5d) similar to the sound wave; the middle part of the reflected wave is noticeably scattered from the surface of the heater and then both waves are propagated in the radial direction. The incidence of such a temperature wave on the boundary leads to the excitation of a compressional sound wave in the vapor (Fig. 5e-5j) and the temperature wave reflected from the boundary remains a density wave. (The direction of the density change in the sound wave is reversed upon reflection from the boundary.) Even in this case, new cylindrical waves are created on the "line" of intersection of the boundary with the wall at the moment of the incidence of the temperature wave from the liquid. A secondary cylindrical wave of second sound is excited in the liquid and is easily distinguished in Figs. 5h-5j by the positive density gradient and the shape of the circular arc. In the photographs here, however, it is not possible to make clear whether this increase in density takes place at the beginning or at the end of the secondary temperature wave. In the vapor phase, a very weak second sound wave is observed, the sign of which is also not clear.

In Figs. 5k-5m, the transformation at the vapor-liquid boundary of the cylindrical sound wave is shown. This is excited in the vapor by heater 15, which is not located above the liquid level. The compressional wave in the liquid is also accompanied by a wave reflected from the wall and reflected waves are propagated after incidence of the waves on the boundary in the vapor phase; sound and temperature waves are excited in the liquid. The refracted sound waves in the liquid are very weak and are partially observed in Fig. 5k in the form of spreading perturbations around the wall. The excited waves of second sound are clearly seen in Figs. 5l and 5m in the region of small angles of incidence. Here the appearance of secondary temperature waves is again observed; these are created on the "line" of contact of the boundary with the wall at the moment of incidence of the sound wave from the vapor. We did not succeed in observing the secondary wave in the vapor in this case, possibly because of the strong perturbation of the vapor around the not yet cooled heater. It must be noted that the front of the secondary waves is nearly a circular cylinder and its intensity is not the same in all radial directions; it falls to vanishingly small values as the vapor-liquid boundary is approached.

4. DISCUSSION OF THE RESULTS

Little information is available about non-stationary processes in liquid helium near the surface of the flat heater in which pulsed emission of Joule heat takes place. The unclear state of the helium around the heater at high heat current density makes the calculation of these processes difficult; an empirical study of heat exchange has been performed only in the study state. The spatial structure of the density perturbations shown in Figs. 2-4, which propagate from the heater without signs of dissipation and nonlinear distortions, can be regarded as information, stretched out in time, concerning processes taking place in the helium near the surface of the heater. At a heater ribbon thickness $2\delta = 0.02$ mm and at a thermal conductivity of constantan $\chi_c = \kappa_c \rho_c C_c \approx 3.3$ cm^2/sec in the range $2-5^\circ K$ (heat capacity $C_c = \psi T \approx 10^{-4} T$[J/g-deg][13], the characteristic time of temperature equalization over the ribbon thickness is equal to $\delta^2/\chi_c \approx 0.3$ μsec. Being interested in time intervals > 1 μsec, one can consider as small the temperature gradient inside the ribbon and the rise time of the electric pulse.

Even in the scarcely noticeable sound perturbations excited by the heater under such conditions, the *visible* leading edge begins with an increase in the liquid density over the entire range of temperatures, independent of the sign of the thermal expansion coefficient, which bears witness to the pressure jump near the heater as the result of local heating of the liquid above

T_ρ or boiling. With decrease in the temperature below T_λ as a consequence of the sharply increasing "thermal conductivity" of the liquid, one should expect a smaller increase in the temperature around the heater, even at the same heat flow. This feature of He II, and also the increasing thermal resistance of Kapitza[1] for finite heat capacity of the heater, can explain the decrease in the intensity and frequency of the sound waves for $T < T_\lambda$, but the reasons for the change of structure of the sound packet and the appearance of the secondary front (Fig. 3) remain unclear.

Taking into account the fact that the structure of the sound packets shown in Figs. 2c-2e is formed only for $N \geq 3$ W/cm^2, it is useful to estimate the conditions for rapid formation of the vapor phase on the surface of the heater. In the experiments conducted, it was established that for $T \gtrsim T_\lambda$, a sharp and intense sound packet arises if the heat ≥ 15 μJ/cm^2 and is released in a time interval ≥ 5 μsec. Without knowing the character of the pulsed heat exchange, it is impossible to compute the flow of heat to the liquid and only approximate estimates are possible. The depth of penetration of heat in the liquid in a time $t = 5$ μsec for $T = 2.2°$K is equal to $\sim \sqrt{\lambda t} \approx 0.4$ μ ($C = 4$ J/g-deg, $\kappa = 2 \times 10^{-4}$ W/cm-deg). Then, from the limiting cases of heat distribution (15 μ J/cm^2) between the heater and the liquid to the end of the pulse, it follows that increase in the heater temperature (with account of the growth of its heat capacity) will be $0.6 \text{ deg} < T_h < 3.5$ deg, where the lower limit corresponds to equality of the temperature of the liquid and the heater ($\Delta T_l = \Delta T_h$) and the upper, $\Delta T_l = 0$ (it is clear that $0 < \Delta T_l < 0.6$ deg).

In spite of the very small heat capacity of the heater (in comparison with the liquid), a lag in the instant of appearance of the visible boundary of the sound packet relative to the beginning of the pulse is noted. (A decrease of the lag with increase of N has also been verified on the photographs of two sound fronts excited simultaneously by heaters 12 and 15, but with different N). The lag indicates that $\Delta T_h \gg \Delta T_l$, and the intense delivery of heat to the liquid occurs only for very high heater temperature, which is produced by the Joule heat at the beginning of the pulse. For $T \gtrsim T_\lambda$ and $N = 3$ W/cm^2, the lag is equal to ~ 3.5 μsec, i.e., it can be assumed that at the end of a pulse ~ 10 μ J/cm^2 remains in the mass of the heater ($\Delta T_h = 2.7°$) and about 5 μJ/cm^2 goes into the liquid. Heating of the liquid at the penetration depth would then amount to only 0.2°, which corresponds to an increase in the equilibrium vapor pressure $\Delta P = 3 \times 10^4$ dynes/cm^2 (~ 23 mm Hg). Upon boiling of the liquid at the surface of the heater, a vapor layer of thickness ~ 1 μ should be formed (the heat of vaporization is 23 J/g, the vapor density is 1.8×10^{-3} g/cm^3) and the displacement of the liquid surface associated with it under the vapor pressure jump, according to the estimates, that is close to ΔP. Increase in the gradients in the sound packet shows that the boiling takes place very energetically in 1-3 μsec.

After cessation of the current, the heater still furnishes heat for a time that is commensurate with the lag, so that the extension of the packet corresponds to the duration of the pulse. Subsequent condensation of the vapor, especially if it fills metastable bubbles of diameter $d = 4\sigma/\Delta P^2 = 0.4$ ($\sigma = 0.3$ dynes/cm is the surface tension of the liquid), produces a smooth rarefaction in the liquid behind the packet (Fig. 2e). In He II, the heat flow that can be taken by the liquid without boiling increases significantly (in the steady state[14], from $W = 0.2$ W/cm^2 for $T \lesssim T_\lambda$ to 2-3 W/cm^2 for $T = 1.9°$K), and the cessation of boiling of the liquid at the surface of the heater may be the cause of the change in the structure of the sound packet for $T < 2.14°$K and $N = 3$ W/cm^2, which becomes similar to the structure of the weak perturbations (see Fig. 2b and Fig. 4c). In the intermediate region $2.14°\text{K} < T < T_\lambda$, the produced vapor phase is rapidly condensed after cessation of heating and it is probable that the appearance of a "secondary" sound front (Fig. 3) corresponds to the "moment of collapse" of the vapor cavities. Then Fig. 7 illustrates the "lifetime" of a vapor bubble in He II as a function of pulse length and temperature for $N = 3.2$ W/cm^2. However, the possibility is not excluded that the secondary front is associated with the formation of the packet of second sound.

Clear vapor cavities are seen in the photographs only for $Nt_* > 100$ μ J/cm^2, for example, the strongly thickened projection of the heater 15 in Figs. 5c-5j. But there is indirect evidence of the long duration of a vapor bubble on the surface of the heater 12 for $T \gtrsim T_\lambda$ and $Nt_* \approx 50$ μ J/cm^2: about 400 μsec after the end of the pulse, incidence of the compressional front, reflected from the wall, on the plane of the heater gives a reflected rarefaction front, as from a vapor-liquid boundary, in addition to a transmitted front.

The described phenomena support the thesis that attempts to obtain intense packets of second sound with pulse power on the surface of the heater $N > 3$-8 W/cm^2 ($T = 2.17° - 1.3°$K) lead to boiling of the liquid, and the shape and intensity of the packet excited in this case through a layer of vapor, are not directly connected with the initial electrical pulse. Osborne[15] excited "shock waves" of second sound with current density in the wave $W = 3.5$ W/cm^2, while the surface of the wire heater (wire of diameter 80 μ and thickness 10 cm) always amounted to 25% of the area of the cross section of the tube and, consequently, $N = 14$ W/cm^2 ($t_* = 10^2 - 10^3$ μsec). If we take it into account that the wires occupy only 8% of the cross section and excite cylindrical waves which do not have a trailing edge, then it scarcely makes sense to associate the "anomaly" of shape of signal at the thermometer, observed by Osborne, with nonlinear effects. Dessler and Fairbank[4] observed a distortion of the shape of the signal upon replacement of the film heater by a wire, explaining this in terms of local heater of the liquid above T_λ.

Packets of second sound, photographed in the absence of evidence of boiling (Fig. 5a) have a much shorter zone of change of density (and temperature) at the trailing edge, in comparison with that of the leading edge, although nonlinear effects in the range 0.9—2°K should produce an increase in the curvature of the leading edge;[16] moreover, they did not succeed in distorting the packet shape in the small time following the instant of its formation. The observed shape of

the packet can be explained, at least in part, by the development of the nonlinear process of heat exchange between the heater and He II for a finite heat capacity of the heater. Experimental values of the current density in the case of stationary heat exchange in He II with large temperature differences, but without boiling, are described by the equation $W = \zeta (T_h^4 - T^4)$, where $\zeta = (1\text{-}2) \times 10^{-2}$ W/cm^2-deg^4[14]. Making use of this equation for the pulse regime, we can estimate the time for establishing the temperature of the heater T_h, assuming that the heat flow in He II is propagated (in two directions) with the speed of second sound, i.e., $W = 2\rho Cu_2 \Delta T_l$ and consequently, $\Delta T_l \ll \Delta T_h$. Neglecting the energy of the wave of first sound, it is necessary to solve the equation of thermal balance $N = g\psi T_h (dT_h/dt) + \zeta (T_h^4 - T^4)$ for two initial conditions: 1) at the moment $t = 0$ the constant power N begins to be released, and $T_h = T$; 2) at $t = 0$, $T_h = T_{h*} > T$, but $N = 0$ always.

Solution shows that at the beginning of the pulse, a smooth increase in temperature takes place, as $t_* \to \infty$, $\Delta T_{l\infty} = N/2\rho Cu_2$ and $\Delta T_{h\infty} = \sqrt[4]{T^4 + N/\zeta}$, and the largest temperature gradient appears in the process of cooling of the heater after the current ceases. The time interval, at the end of which $T_h \approx 0.95\ T_{h\infty}$, is obtained from solution equal to ~7 μsec for $T = 2.0$°K and $N = 3$ W/cm^2 and increases several fold with decrease in T and N. The absolute width of the bands at the fronts of the packet (Fig. 5a) is not known exactly, in view of the possible diffraction of the light, but corresponds tentatively to times of the order of 20-50 μsec. It is quite probable that there is another mechanism which controls the different structure of the boundaries of the packet of second sound. Estimates that have been made give for pulsed heat exchange, $T \gtrless T_\lambda$, values of the heat exchange coefficients that are close to those observed under stationary conditions.

Interest is created by secondary cylindrical waves, which are created on the "lines" with physical singularities at the moment of passage of the front of the packet. On the cross-sections of the plane of the heater 12 with the horizontal walls (Figs. 2–4) the conditions for the appearance of such waves are complicated by the presence of gaps (0.1 mm) between which are the ribbons of the heater. The gap, made at the low right hand corner of Fig. 5c, in the reflection of the cylindrical sound wave give a similar picture, for which several secondary waves are characteristic (see Fig. 2b), formed evidently as a consequence of the motion of the liquid in the gap and resonance phenomena in the cavity behind the gap. The simplest condition are obtained in the intersection of the heater 12 with the vapor-liquid boundary (Figs. 4a and 4b), but even in this case the line of contact is discontinuous and it is not possible to exclude the possibility of any singularities in the release of heat. However, it is clear that the upper layer of the liquid on this line possesses greater mobility than the liquid at greater depths, and therefore the pressure jumps in the liquid, which exceed the changes in the vapor, create cylindrical waves of opposite sign. They accompany amplification of the intensity of the rarefaction sound waves in this case (Fig. 4a) and more favorable possibilities for boiling of the liquid on the vapor boundary.

Extremely pure conditions apply on the "line" of contact of the vapor-liquid boundary with the plane, smooth vertical wall, when the wave packet excited elsewhere is incident on this line (Figs. 5c-m). The secondary waves in this case evidently arise as the result of scattering of incident waves on the surface of the liquid meniscus wetting the wall.

The author is very grateful to P. L. Kapitza, A. F. Andreev, and V. P. Peshkov for discussion of this research.

[1] P. L. Kapitza, Zh. Eksp. Teor. Fiz. 11, 1 (1941).
[2] V. P. Peshkov, Zh. Eksp. Teor. Fiz. 16, 1000 (1946).
[3] J. R. Pellam, Phys. Rev. 75, 1183 (1949).
[4] A. J. Dessler and W. M. Fairbank, Phys. Rev. 104, 6 (1958).
[5] A. I. Gulyaev, ZhETF Pis. Red. 5, 399 (1967) [JETP Lett. 5, 279 (1967)].
[6] S. A. Abrukov, Tenevye i interferentsionnye metody issledovaniya opticheskikh neodnorodnostei (Shadow and Interference Methods of Investigation of Optical Inhomogeneities) (Kazan' State Univ. Press, Kazan', 1962).
[7] K. R. Atkins, Liquid Helium (Cambridge Univ. Press, 1959).
[8] E. G. Kerr and R. D. Taylor, Ann. Phys. 26, 292 (1964).
[9] V. P. Peshkov and A. P. Borovikov, Zh. Eksp. Teor. Fiz. 50, 844 (1966) [Sov. Phys.-JETP 23, 559 (1966)].
[10] K. R. Atkins and C. E. Chase, Proc. Phys. Soc. (London) A64, 826 (1954).
[11] V. P. Peshkov, Zh. Eksp. Teor. Fiz. 38, 799 (1960) [Sov. Phys.-JETP 11, 580 (1960)].
[12] D. M. Chernikova, Zh. Eksp. Teor. Fiz. 47, 537 (1964) [Sov. Phys.-JETP 20, 358 (1965)].
[13] W. Keesom and B. Kurrelmeyer, Physica 7, 1003 (1940).
[14] B. W. Clement and T. H. K. Frederking, Bull. Inst. Int. Froid, Annexe, 1966-5, p. 49.
[15] D. V. Osborne, Proc. Phys. Soc. (London) A64, 114 (1951).
[16] I. M. Khalatnikov, Zh. Eksp. Teor. Fiz. 23, 253 (1952).

Translated by R. T. Beyer
9